Astron. Astrophys. 315, L141–L144 (1996)

ASTRONOMY
AND
ASTROPHYSICS

ISOCAM 4 μm imaging of the nuclear starburst in M83*

D. Rouan[1], **D. Tiphène**[1], **F. Lacombe**[1], **O. Boulade**[2], **J. Clavel**[3], **P. Gallais**[2], **L. Metcalfe**[3], **A. Pollock**[3], **and R. Siebenmorgen**[3]

[1] Observatoire de Paris-Meudon, Département Spatial, CNRS, F-92195 Meudon Cedex, France
[2] CEA Service d'Astrophysique, CEN Saclay, F-91191 Gif-sur-Yvette, France
[3] ISO SOC, ESA, Villafranca, P.O. Box 50727, E-28080 Madrid, Spain

Received 18 July 1996 / Accepted 19 August 1996

Abstract. We present ISOCAM images (1.5 arcsec resolution), in the Brα line and in the continuum at 4 μm, of the starburst nuclear region in the nearby galaxy M83. The starburst is found to lie: a) along arc joining the 2 μm sources at S and SW of the nucleus to the NW 10 μm peak, a possible indication of a propagating star formation; b) at the nucleus itself and at a bridge, linking the arc to the nucleus, that could trace a gaseous bar. The strong 4 μm continuum emission cannot be free-free and probably corresponds to the continuum emission associated with the Very-Small-Grain/PAH component of the dust.

Key words: galaxies: individual: M83 – galaxies: starburst – infrared: ISM: continuum, lines and bands

1. Introduction

Nuclear starburst activity is frequently associated to barred spiral galaxies and/or interacting galaxies (e.g. Hawarden et al., 1986, Wynn-Williams, 1987): it is very likely the consequence of the huge concentration of gas that has been driven to the centre of the galaxy thanks to non axisymmetric gravitational torques induced either by the stellar bar or by the second galaxy. Dynamical models have fully confirmed this view (Barnes & Hernquist, 1992). The magnitude of the burst may vary by a large factor (Telesco, 1988), the IR luminosity spanning a range 10^9 – $10^{12} L_\odot$, when going, for instance, from enhanced star formation in the central 1 kpc of the Milky way to the Ultra Luminous IRAS galaxies. Understanding the exact nature of the mechanism that governs the magnitude of the burst in the central regions of galaxies and the way it may propagate, are important issues because they relate to the more general questions of the origin of the AGNs and their occurence since Sanders et al.(1988) proposed that the most important starburst are likely the progenitor of AGNs. The exact nature of the relationship between the two types of activity is still to establish, but clearly, studies at infrared wavelength represent a key tool to obtain new clues: a) it is possible to probe those heavily obscured regions; b) the far-IR luminosity traces the stellar luminosity through the dust thermal emission; c) near- and mid-IR radiations give complementary information on the stellar photospheric emission and on the nebular emission from the ionized gas. Imaging at a good angular resolution is needed to establish the potential link between the different components that may be involved – stellar nucleus, large HII/H_2 complexes, ring of starburst, AGN – since the typical scale of a starburst nuclear region is 50 – 500 pc, i.e. 1" – 10" at 10 Mpc.

The wavelength range 3-10 μm is a peculiar one since it corresponds to the transition to a flux dominated by dust radiation. Because of the opacity of the atmosphere and the huge background, very few observations in that range were done from the gound; this is however a spectrally rich region (3.05 ice feature, "PAH" bands, Brackett lines, free-free, dust emission). Obviously ISO will fill a large gap in opening widely this window.

M83 (NGC 5236) is the nearest (at 3.7 Mpc) face-on barred spiral galaxy(SABc). Strong emision in X-Ray (Trinchieri et al., 1985), UV (Bohlin et al., 1990), near-IR (Gallais et al., 1991, hereafter GRLTV), mid-infrared (Telesco et al., 1988), radio (Condon et al., 1982; Cowan, Roberts & Branch, 1994) and CO (Handa et al., 1990) is indicative of a star burst in the $\approx$ 300 pc central region. The burst is rather strong: L = 4 10^9 $L_\odot$ for the nuclear region (i.e. one sixth of M82), 13 10^9 $L_\odot$ for the whole galaxy, and is characterized by a high surface brightness (I $\approx$ 3.5 10^5 $L_\odot pc^{-2}$) corresponding to hot-spots at $\approx$ 100–200 pc from the nucleus. This very short distance of what is likely the location of the Inner Linblad Resonance, suggests that a strong concentration of molecular gas is present at the center of M83, as confirmed by CO measurements. GRLTV

Send offprint requests to: D. Rouan (rouan@obspm.fr)

* ISO is an ESA project with instruments funded by ESA Member States (especially the PI countries: France, Germany, the Netherlands and the United Kingdom) and with the participation of ISAS and NASA. We thank all the members of the ISOCAM team for their unvaluable work, with a special mention to M. Arfouillaud, G. Epstein, R. Knoll, J.P. Mengué, P. Puget, J.P. Rivet, D. Stefanovitch, B. Talureau, P. van Duoc who have been deeply involved in the development of the CAM-SW channel.

showed that the starburst region can be described by three main components : *i)* a stellar nucleus, well identified in the near-IR; *ii)* an arc of emission (reminiscent of a complete ring ?), perpendicular to the bar and at a distance of $\approx$ 100 pc from the nucleus; *iii)* a bridge of fainter emission linking the nucleus and the arc along the direction of the bar. We present, in the following, the study we made of the whole nuclear region at 3.88 μm (continuum) and in the Brα line (4.06 μm), using the SW channel of ISOCAM. At this wavelength, the exact origin of the continuum emission is not obvious and we will discuss different cases: nebular emission from the HII regions (free-free mainly), stellar photospheric emission, thermal emission from Very Small Grains. Observations and data processing are described in section 2 and the results and their dicussion in section 3.

2. Observations and Data Processing

The observations, performed with the short wavelength channel of ISOCAM (Cesarsky et al., 1996), the camera onboard ISO (Kesslet et al., 1996) , took place at the very end of the Preliminary Verification (PV) phase of ISO in January 1996. The pixel field of view was 1.5 arcsec and the observations done successively in three filters: SW6, SW8 (Brα) and SW9 (3.88 μm), with an integration time per frame of 20 sec. Because the detector has been switched on at the very beginning of the sequence, a warm-up drift, probably due to the cold electronics nearby the array, severly hampered the first part of the observation: we present here only the last sequences corresponding to the SW8 and SW9 filters. The pointing stability on ISO has been shown to be much better than specified and indeed, the image quality appears practically not degraded by the random angular motion of the satellite.

The most important artefact on the image comes from the warm-up drift of the bias signal which, on the average, translates into a nearly exponential decrease of the signal towards the dark level. Unfortunately, this effect has a non-uniform behaviour accross the array: the bias voltage of each pixel evolutes in a different way from one to the other and there is no simple offset or scaling law able to reproduce the difference of behaviour between pixels. However, a grid structure, with a pattern reproduced each 3 row, is clearly seen. To remove this artefact, we have adopted the following procedure: *i)* a vector, median of the rows, is computed, to evaluate the spurious pattern along the row direction; *ii)* this vector is then zero-centered (mean substracted to all components); *iii)* this median, zero-centered, vector is substracted with a proper weight to each row. Since the spurious signal appears as a noise correlated between rows, the weight is computed so as to minimize the cross-correlation coefficient between each row and the “spurious" vector. One can show that the cross-correlation coefficient vanishes when the weight is $\boldsymbol{V_{sp}} \cdot \boldsymbol{V_i}/(|\boldsymbol{V_{sp}}||\boldsymbol{V_{sp}}|)$, where $\boldsymbol{V_{sp}}$ and $\boldsymbol{V_i}$ are respectively the “spurious" vector and the row vector. Since the average value of the “spurious" vector is zero, this procedure does not affect the total flux. In order to check that this processing does improve the quality of the data and does not introduce too many artefacts, we have used it on the observation of another galactic nucleus, M51, for which the same field has been observed with the LW channel of CAM: there is indeed a very good correpondance between the two images. We did not apply a flat-field correction, but zodiacal light does not contribute too much to the background at those wavelength, and the contrast of the image is rather important; however, in order to smooth the high frequency pixel-to-pixel differential response, the image was finally smoothed using a convolution by a 3$\times$3 pattern (1 at center, .2 elsewhere). Calibration of the images was done using the output of the PV phase general calibration measurement.

3. Results and discussion

The resulting images are presented on Fig. 1, together with the 2.2 μm image obtained by GRLTV. Despite the fact that the nucleus is not well centered on the array and, thus, that part of the extended emission is missing, several features are unambiguously identified, thanks to the comparison with the near-IR images of GRLTV: a) the nucleus, that still appears as the brightest source at 4.0 μm; b) a bow-shaped circumnuclear region at West, but with an extension to the NW more important than at 2 μm, especially in the Brα line; c) a bridge of emission linking the nucleus to the arc and which appears, here, more prominent than at shorter wavelength, with an extension beyond the arc, outward in the bar direction. We now discuss the nature and characteristics of those different components.

3.1. Nucleus

Assuming that extinction is negligible at 4 μm, we derive the flux of the nucleus (brightest pixel) – above the background emission – $\approx$ 2.9 10^{-13} erg cm^{-2} s^{-1} in the Brα line and 11 mJy in the continuum at 3.88 μm. The strong Brα emission is clearly peaking on the nucleus, since the brightness is 2 times larger than in a 7.2 arcsec diaphragm (Turner, Ho and Beck, 1987). The star formation must be very efficient at this location: indeed, assuming a negligible extinction at 4 μm, and converting Brα luminosity to ionizing photons gives: N_{Lyc} = 1.1 10^{52} s^{-1}, which would correspond to $\approx$ 4.9 $10^8 L_\odot$ (Mezger et al., 1974) in a region of $\approx$ 30 pc in diameter, i.e. a brightness comparable to giant HII complexes in the Milky Way; of course, the near-IR images suggest that the actual surface brightness is likely much higher. This result is apparently in conflict with HST images in the Hα line by Heap et al. (1993) who conclude that the nucleus is not a source of Hα emission; however the extinction which must affect the whole region (Turner et al., 1987) could explain the discrepancy. Using the photometry by GRLTV, we find that the color index (K-SW9) of the nucleus is 0.75. This is much redder than what any stellar photosphere can account for, but is lower than the (K-SW9) = 1.16 that would be given by pure free-free emission. If we assume that this index is entirely due to reddened starlight, we derive $A_{\rm v}$ $\approx$ 13 mag, at least towards the stars at the periphery of the starburst. If the IR excess is rather a mixing of reddened starlight and of nebular emission from H^+, it remains

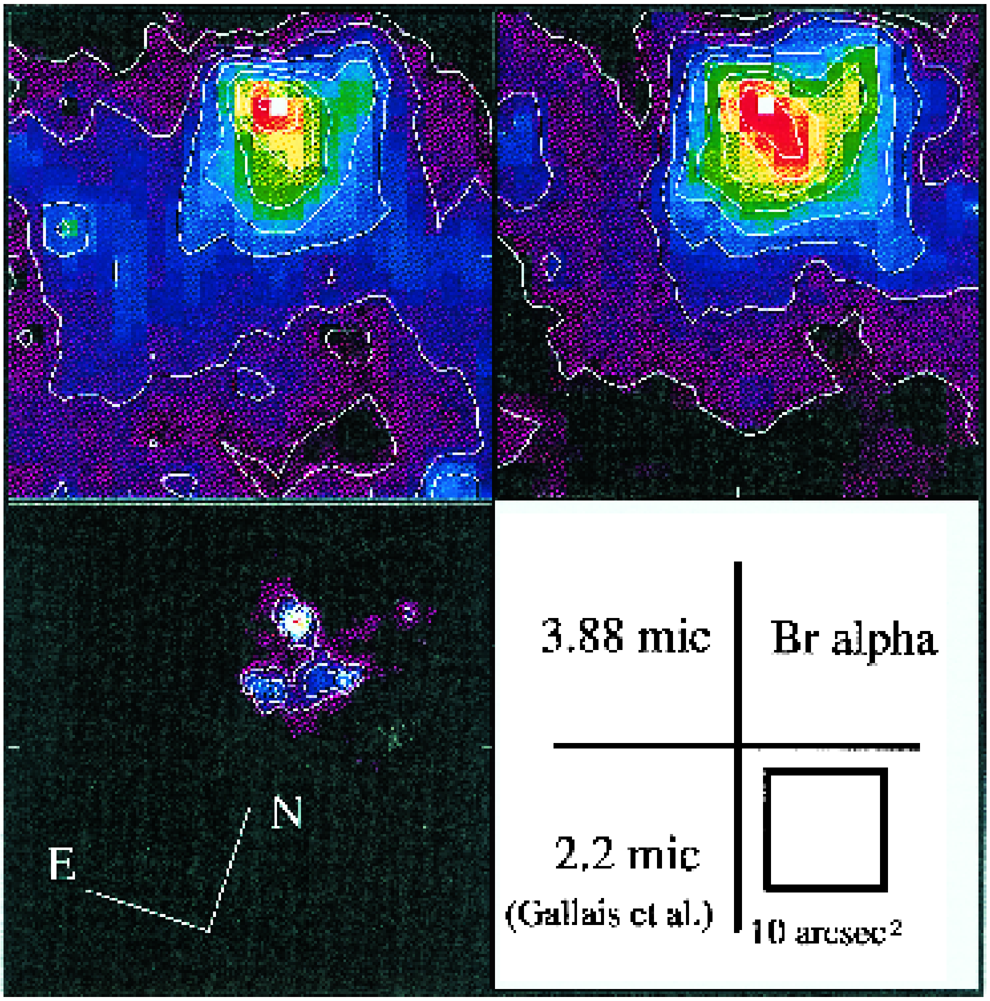

Fig. 1. From upper right to down left: Brα, 3.88 μm continuum and 2.2 μm images of the central region of M83; the two first have been obtained with the SW channel of CAM and the third one is taken from GRLTV. The false color scale is adjusted so as the lowest contour is 1 σ below the median value which corresponds to an underlying smooth emission and some residual bias offset. The highest contours on the first two images correspond respectively to 17.8 and 7.6 mJy $('')^{-2}$ and the interval between two contours to 1.33 and 0.62 mJy $('')^{-2}$

an indication that the nucleus is, by itself, an active star forming region, may be the most prominent one.

3.2. The starburst arc

At 4 μm, and especially in the Brα line, the arc of emission seen in the near-IR is well defined. It probably defines the Inner Linblad Resonance where the gas should accumulates under the action of the bar (GRLTV). At a projected distance of $\approx$ 100 pc from the nucleus, it extends on $\approx$ 450 pc from South to NW, linking in fact the regions which are prominent at 2 μm to the ones which are dominating in the 10 μm image, i.e. at $\approx$ 12 arcsec NW to the nucleus. If we consider that the 10 μm peak must be associated to the most active site of star formation, albeit deeply enshrouded in the dust, then we may suppose that it is also the most recent one, the matter of the parental cloud having not yet been blown-out by the SN explosions. The striking connection at 4 μm between the presumably older 2 μm regions and the very young star forming region strongly suggest that *a mechanism of chain reaction, traced by the 4 μm emission, has been in action along the molecular belt.* Why does the 4 μm image not peak at the same location as the 10 μm map ? this is probably an indication that the opacity is so large in the youngest region, that only a fraction of the 4 μm radiation can escape. A rough estimate indicates opacities in excess of 50 mag at this location. We have evaluated the input stellar luminosity that could account for the 3.88 μm continuum emission in the brightest area of 15 arcsec diameter, assuming that the main source of radiation is either photospheric stellar emission, or free-free continuum from the HII regions, or heated dust (assuming classical grains); we find L = 1.0 10^{10} $L_\odot$, 9.1 10^{11} $L_\odot$ and 1.7 10^{13} $L_\odot$ respectively (for a dust temperature of 160 K in the latter case). All those values appear unreasonably high. On the other hand, the K-SW9 colour index ranges between .7 and 1.2, indicating either a very important reddening or a non stellar red emission. We think that the most plausible origin of the 4 μm flux could be the *continuum emission from the PAH / Very Small Grains component* which has been shown recently to contribute very significantly at those wavelengths (see Bernard et al., 1994 for the Milky Way; Sellgren et al., 1985 for reflection nebulae and Normand et al., 1995 for M82). The model of Very Small Grains in the ISM by Désert et al. (1990) gives a ratio $(\nu I_\nu)_{4\mu m}/(\nu I_\nu)_{2\mu m} \approx 1.4$, while we find a ratio of $\approx$ 1.0 for the brightest 2 μm region of the arc: this is a reasonable agreement in view of the uncertainties.

3.3. The bridge

This structure was only apparent on near-IR images as a faint emission linking the nucleus to the arc, along the same direction as the bar. At four microns, it appears now as a bright ridge, in fact the brightest region when one exclude the nucleus, as evidenced by the contour plot on Fig. 1. It has been proposed by Schlosman et al., 1989, that a possible mechanism for providing – through nonaxisymmetric torques – the nucleus with fresh matter from the molecular ring, could be the existence of a gaseous "bar within the bar". Indeed, the fact that the nucleus itself appears as an active site of star formation, requires that it is – or has been recently – fed with important quantities of gas; we suggest that the bridge we observe can be the trace of such a gaseous "bar within the bar". The exact origin of the IR radiation at 4 μm is however not clear: it corresponds to an important IR excess (K-SW9 = 2.3) and a strong Brα emission but has no major strong counterpart at 10 and 2 μm, rather a faint ridge in each case. On the other hand, one notes that M83 does exhibit the signs of highly energetic processes, revealed by the X activity and a fast velocity wind (Bohlin et al., 1990). A tentative and speculative explanation could be that very small grains or PAHs are heated by some high energy particles.

4. Conclusion

To summarize the main results: a) The 4 μm maps share morphological structures with both the 10 μm and the 2 μm images, especially an arc joining the 2 μm sources at S and SW of the nucleus to the NW 10 μm peak. We argue that this is an indication that the star forming activity has propagated according to a chain reaction all along the arc. b) The starburst is not confined to the arc only: it shows also at the nucleus and along a bridge linking the arc to the nucleus; this appears rather unexpected since it is generally thought that transport of gas to the very central region, .i.e. inside the theoretical limit of the ILR, requires a loss of angular momentum that no simple mechanism is able to provide. c) We suggest that the bridge traces a gaseous bar that may be responsible of the required torques, as proposed on theoretical grounds. d) If the 4 μm continuum emission is certainly a tracer of the starburst, its origin cannot be dust emission, nor free-free emission from the ionized gas. We rather propose that it corresponds to the continuum emission associated with the Very-Small-Grain/PAH component of the dust.

References

Barnes J.E., Hernquist L., 1992, ARA&A 30, 705
Bernard J.P. et al., 1994, A&A 291, L5
Bohlin R.C. et al., 1990, ApJ 363, 154
Ceśarsky C. et al., 1996, A&A, this issue.
Condon J.J. et al., 1982, ApJ 252, 102
Cowan J.J., Roberts D.A. & Branch D, 1994, ApJ 434, 128
Désert F.X., Boulanger F., Puget J.L., A&A 237, 215
Gallais P., et al., 1991, A&A 243, 309 (GRLTV)
Handa T. et al., 1990, PASJ 42, 1
Hawarden T.G. et al., 1986, MNRAS 221, 41p
Heap S.R. et al., 1993, BAAS, 182, 31.04
Kessler M., et al., 1996, A&A, this issue
Mezger P.G., Smith L.F., Churchwell E., 1974, A&A 32, 269
Normand P., 1995, A&A 297, 311
Sanders D.B. et al., 1988, ApJ 325, 74
Sellgren K. et al., 1985, ApJ 299, 416
Schlosman I., Frank J., Begelman M.C., 1989, Nat 338, 45
Telesco C.M., 1988, ARA&A 26, 343
Trinchieri G. et al., 1985, ApJ 290, 96
Turner J.L., Ho T.P., Beck S.C., 1987, ApJ 313, 644
Telesco C.M., Gatley I., 1984, ApJ 284, 557
Wynn-Williams C.G., 1987, in *Star Forming Region*, IAU Symp. No 115, eds M. Peimbert, J. Jugaku, p.587.